Regular article

Particles collision near regular charged black holes

Pameli Saha [1] · **Ujjal Debnath** [2]

[1] Department of Mathematics, Indian Institute of Engineering
Science and Technology, Shibpur, Howrah-711 103, India.
email: pameli.saha15@gmail.com

[2] Department of Mathematics, Indian Institute of Engineering
Science and Technology, Shibpur, Howrah-711 103, India.
Corresponding author email: ujjaldebnath@gmail.com

Abstract. In this work, we consider a static spherically symmetric charged regular black hole to investigate arbitrarily high center of mass-energy near the horizon with particle collision for extremal case in the equatorial plane ($\theta = \pi/2$). Here we also study circular geodesics and find the ISCO and MBCO radii. We analyze the two neutral particles collision with the same masses and different masses. Also, we analyze the particle collision with massless photon and photon-photon collision near the horizon of this regular black hole to calculate the center-of-mass energy.

Keywords: Collision; Black hole; Horizon.

1   Introduction

Black holes are important objects from a holographic point of view. Also, AdS/CFT correspondence can understand particle collisions of LHC or RHIC. In this paper, we would like to consider a regular charged black hole as the particle accelerator. In 2009, Banados, Silk, and West [1] perceived that two particles falling from rest at infinity into the Kerr black hole's horizon may crash with arbitrary high center-of-mass (CM) energies near the event horizon in the equatorial plane ($\theta = \frac{\pi}{2}$) if the critical angular momentum of one of the particles close to the angular momentum of marginally bound geodesics and maximum spinning of the black hole. This procedure of acceleration of particles with a black hole is known as the BSW mechanism. In 2010, Jacobson and Sotiriou [2] discussed the CM energy for non-extremal Kerr Black Hole. In that year, Lake [3] also identified the divergence of CM energy at the inner horizon of Kerr Black Hole for the non-extremal case. Also, CM energy of rotating black hole was discussed by Zaslavskii [4]. Wei et al. [5] investigated the CM energy of the charged spinning black hole in which the CM energy is to be controlled by the spin and charge parameters. After, Li et al [6] studied high center-of-mass energy for the Kerr-(anti) de Sitter Black Hole. Liu et al. [7] also revealed the CM energy of Kerr-Taub-NUT Black Hole at the horizons. [8] described BSW mechanism for general stationary charged black hole. Said and Adami [9] carried out the particle acceleration for a rotating charged cylindrical black hole. Many authors recently examined black hole particle acceleration in [10, 11, 12, 13, 14, 15]. A brief review on the black hole as particle accelerator has been discussed in [16].

Now, geodesics of the black hole as a particle accelerator was catching the attention of many authors. Recently, Pradhan [17] studied the geodesics of regular black holes. Abbas [18] and Bambi [19] also discussed the same topic. The circular orbits satisfying $r > r_{ISCO}$ are stable and unstable when $r < r_{ISCO}$, r_{ISCO} is the radius of Innermost Stable Circular orbit (ISCO) and these circular orbits are bounded with $r < r_{MBCO}$, r_{MBCO} is the radius of Marginally Bound Circular Orbit (MBCO). These orbits are very interesting for black hole study in Astrophysics.

It is well-known that curvature singularities were present in the conventional black holes such as Schwarzschild black hole, Kerr black hole, RN black hole, and Kerr-Newman black hole. Then Physics failed at these singularities. Whenever Penrose's cosmic censorship [20, 21] stated that if General Relativity predicted singularities, they would be dressed up by event horizon; hence, people started to avoid the singularity. Bardeen was the first author who discovered a non-singular black hole modifying RN black hole, which was known as "Bardeen Space-time" or "First Regular Black Hole" [22]. Here the word "Regular" means that the curvature is non-singular or regular everywhere. After, Ayon-Beato et al. [23] discovered a second regular black hole v.z., ABG black hole. Another kind of regular black hole (Hayward black hole) [24] was demonstrated. Amir and Ghosh [25] also investigated the rotating Hayward black hole as a particle accelerator and noticed that center of mass-energy diverges in the vicinity of the horizon for the extremal cases. Saha and Debnath [26] also observed the high center-of-mass energy of coming particles from rest at infinity near the horizon of the charged MSW black hole in $2 + 1$ dimension for the extremal case. Pradhan [27] did the same work for charged dilaton black hole. These types of black holes have a de Sitter center [28]. Recently, Balart and Vegenas [29] have studied a family of regular black hole metrics, which by construction satisfy the Weak Energy Condition (WEC). Similarly, other black hole solutions satisfying WEC have been found in [30, 31, 32]. These regular black holes violate Strong Energy Condition (SEC) but obey the WEC. Many authors have studied different types of regular black holes [33, 34]. The black hole solutions have been derived via the dual representation of nonlinear electrodynamics. They have constructed several charged regular black hole metrics employing mass distribution functions which are inspired by continuous probability distributions. So it will be interesting to study the particles collision for this types of regular charged black holes.

Motivation of our paper is to check the non-divergency or divergency (finite or infinite value) of the CM energy for both non-extremal and extremal cases of a regular charged black hole (chosen from [29]) and make a comparison with the BSW effect like [1, 17, 25, 26, 27]. In section 2, a brief study of a regular charged black hole is given to calculate the radii of outer and inner horizons of our black hole, and we investigate circular geodesics for null and time-like cases to find out the angular momentum and energy per unit mass. For null geodesics, we calculate effective potential and impact factors. We also study ISCO and MBCO radii for our charged regular black hole. Calculation of center of mass-energy for mass particle collision near outer/inner horizon of our black hole is analyzed in section 3. A discussion of center-of-mass energy for particle-photon is given in section 4, photon-photon collision is given in section 5 and section 6 deals with a brief summary of the work done.

2   A flying study of a regular black hole with particles collision

A various types of probability mass function of regular black holes can be constructed from various continuous probability distribution functions in [29] for investigation as particle

accelerators. From several types of regular charged black holes, we assume a static spherically symmetric non-singular (regular) charged black hole as [29]

$$ds^2 = -\mathrm{F}(r)dt^2 + \mathrm{F}(r)^{-1}dr^2 + r^2(d\theta^2 + \sin^2\theta d\phi^2), \tag{1}$$

with

$$\mathrm{F}(r) = 1 - \frac{2M}{r}\left\{\frac{1}{(1+\frac{q^2}{4Mr})^2}\right\}, \tag{2}$$

where M and q denote the Arnowitt-Deser-Misner (ADM) mass and magnetic charge of the regular black hole. A details derivation of the function $\mathrm{F}(r)$ have been obtained in Ref. [29]. For this case, the source to the Einstein field equations corresponds to nonlinear electrodynamics model (coupled to general relativity), which is compatible with the Maxwell weak field limit. We see that there is no curvature singularity, i.e., no singularity at $r = 0$. Now, we get the horizons of this regular black hole if $\mathrm{F}(r) = 0$, which gives [29],

$$r^2 + r\left(\frac{q^2}{2M} - 2M\right) + \frac{q^4}{16M^2} = 0, \tag{3}$$

whereas the horizons are given by

$$r_\pm = \frac{-(\frac{q^2}{2M} - 2M) \pm \sqrt{4M^2 - 2q^2}}{2}.$$

There exist two horizons: Event/Outer horizon for $r = r_+$ and Cauchy/Inner horizon for $r = r_-$ if $M^2 \geq \frac{q^2}{2}$ i.e., $q^2 \leq 2M$. When equality occurs, these two horizons coincide and then it presents an extreme regular black hole. When $q \to 0$ then $r_+ = 2M$ and $r_- = 0$ gives the event horizon (no inner horizon) of Schwarzschild black hole. Here we draw the figure of $\mathrm{F}(r)$ with different behavior in Fig. 1.

3 Equatorial Circular Geodesics

To acquire the complete geodesic structure of our charged regular black hole we should accompany the pioneer book of Chandrasekhar [35] and Hartle [36]. We consider a particle manifesting clearly the geodesics motion in the equatorial plane $\theta = \frac{\pi}{2}$ for which $\dot{\theta} = u^\theta = 0$ where $\mathbf{u} = (u^t, u^r, u^\theta, u^\phi)$ is the four-velocity of the particle and we go after the colonist book of S. Chandrasekhar [35]. Now the Lagrangian of the metric (1) is given by

$$2\mathrm{L} = -\mathrm{F}(r)\dot{t}^2 + (\mathrm{F}(r))^{-1}\dot{r}^2 + r^2\dot{\phi}^2, \tag{4}$$

whereas the generalized momenta tells

$$p_t \equiv \frac{\partial \mathrm{L}}{\partial \dot{t}} = -\mathrm{F}(r)u^t, \tag{5}$$

$$p_r \equiv \frac{\partial \mathrm{L}}{\partial \dot{r}} = (\mathrm{F}(r))^{-1}u^r, \tag{6}$$

$$p_\theta \equiv \frac{\partial \mathrm{L}}{\partial \dot{\theta}} = 0, \tag{7}$$

$$p_\phi \equiv \frac{\partial \mathrm{L}}{\partial \dot{\phi}} = r^2 u^\phi. \tag{8}$$
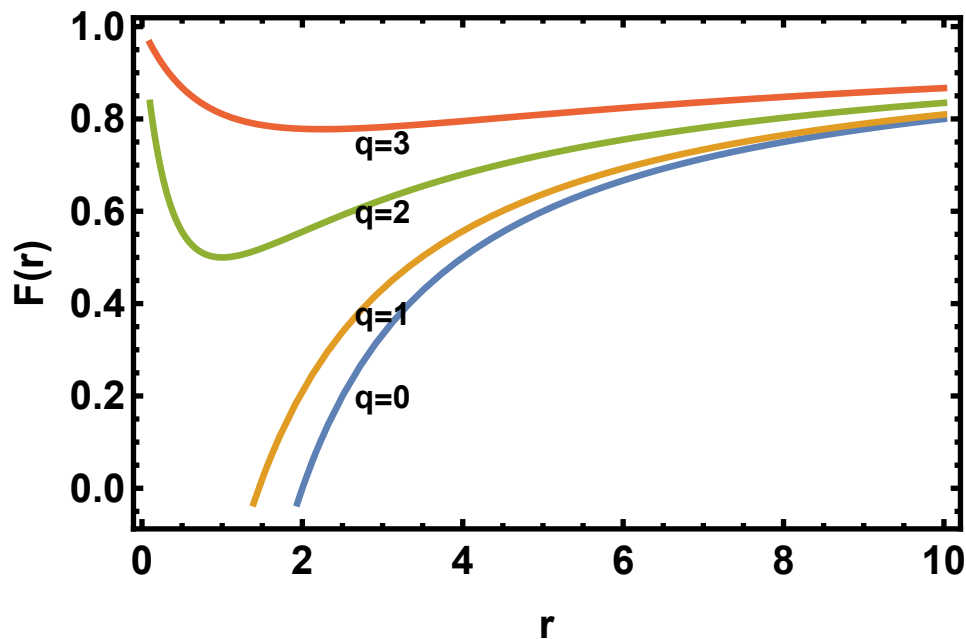
Figure 1: Plots of F(r) for null geodesics w.r.t. r for different values of q. (For interpretation of the references to color in this figure legend, the reader is referred to the web version of this article.)

Here dot denotes the derivative w.r.t. the affine parameter. The conserved energy and angular momentum per unit mass can be defined [37] as in the following form:

$$E = -p_t = \mathrm{F}(r)u^t, \tag{9}$$

$$L = p_\phi = r^2 u^\phi. \tag{10}$$

Solving equations (9) and (10) we obtain

$$u^t = \frac{E}{\mathrm{F}(r)}, \tag{11}$$

$$u^\phi = \frac{L}{r^2}. \tag{12}$$

The Hamiltonian is as

$$\mathrm{H} = p_t u^t + p_r u^r + p_\phi u^\phi - \mathrm{L}. \tag{13}$$

For the Hamiltonian being independent of "t", we write it as

$$2\mathrm{H} = -\mathrm{F}(r)(u^t)^2 + (\mathrm{F}(r))^{-1}(u^r)^2 + r^2(u^\phi)^2 = \sigma, \tag{14}$$

where σ is defined as

$$\sigma = \begin{cases} 0, & \text{for null geodesics,} \\ +1, & \text{for space-like geodesics,} \\ -1, & \text{for time-like geodesics.} \end{cases} \tag{15}$$

Now substituting the equations (11), (12) in equation (14) we obtain the radial equation as [38],

$$(u^r)^2 = E^2 - \mathrm{V}_{eff} = E^2 - \left(\frac{L^2}{r^2} - \sigma\right)\mathrm{F}(r),\tag{16}$$

where the effective potential is

$$\mathrm{V}_{eff} = \left(\frac{L^2}{r^2} - \sigma\right)\mathrm{F}(r).\tag{17}$$

3.1   Null geodesics

Here we take $\sigma = 0$ for the null circular/photon orbits. So the effective potential (17) becomes [38]

$$\mathrm{U}_{eff} = \frac{L^2}{r^2}\mathrm{F}(r) = L^2\left[\frac{1}{r^2} - \frac{32M^3}{r(q^2 + 4Mr)^2}\right].\tag{18}$$
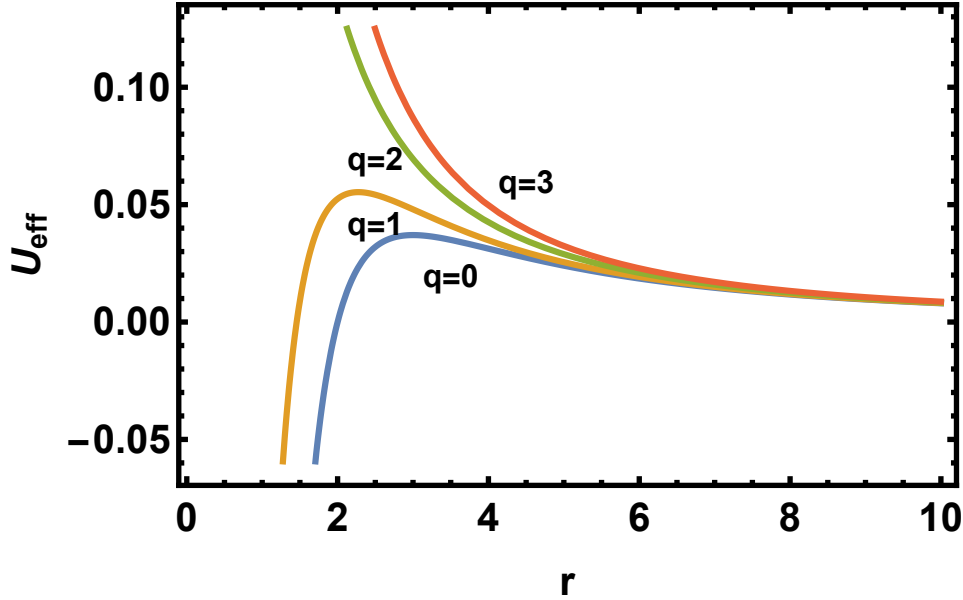
Figure 2: Plots of effective potential U_{eff} for null geodesics w.r.t. r for different values of q. (For interpretation of the references to color in this figure legend, the reader is referred to the web version of this article.)

We have plotted the effective potential (U_{eff}) against radius (r) for different values of q for the null geodesics in Fig. 2. The effective potential reaches zero for non-charged and charged cases for null geodesics. It increases rapidly from negative infinity, crossing zero to a positive value, and then decreases very slowly, tending to zero for $q = 0$ and $q = 1$ with radius. But for $q = 2$ and $q = 3$, the effective potential decreases rapidly from a positive value to reach zero with radius. For photon orbit, we must have

$$\left.\begin{array}{r}U_{eff} = E^2, \\ \frac{dU_{eff}}{dr} = 0.\end{array}\right\}\tag{19}$$

Thus with the help of equation (18), equation (19) reduces to

$$\frac{E}{L} = \pm \frac{\sqrt{(q^2 + 4Mr)^2 - 32M^3r}}{r(q^2 + 4Mr)}, \tag{20}$$

and

$$64M^3r^3 + 12M^2r^2(q^2 + 16M^2) + 4Mq^2r(3q^2 - 4M^2) + q^6 = 0. \tag{21}$$

Solving equation (21), we get the radius of the circular photon orbit of this regular black hole. When $q \to 0$ then $r = 3M$ gives the radius of the photon orbit of the Schwarzschild black hole.

The impact parameter (D_{IF}) which describes the shape of the orbit of a photon incident from infinity on a black hole given as

$$\frac{1}{D_{IF}} = \frac{E}{L} = \frac{\sqrt{(q^2 + 4Mr)^2 - 32M^3r}}{r(q^2 + 4Mr)}. \tag{22}$$

When $q \to 0$ then $D_{IF} = 3\sqrt{3}M$ corresponds to circular photon orbit for the Schwarzschild black hole.

3.2   Time-like geodesics

For time-like geodesics i.e., $\sigma = -1$ the radial equation (16) and effective potential (17) reduce to

$$(u^r)^2 = E^2 - V_{eff} = E^2 - \left(\frac{L^2}{r^2} + 1\right) F(r), \tag{23}$$

and

$$V_{eff} = \left(\frac{L^2}{r^2} + 1\right) F(r). \tag{24}$$

We have plotted the graphs for radial component (u^r) and effective potential (V_{eff}) with respect to radius (r) for time-like geodesics in Fig. 3 and Fig. 4. From Fig. 4, we have noticed that for the non-charged $(q = 0)$ and charged $(q = 1)$ regular black hole, the effective potential reaches zero from negative values, then increases with r. For $q = 2$ and $q = 3$, the effective potential decreases rapidly and then increases asymptotically in positive values with radius. For circular geodesics, we must have

$$\left.\begin{array}{l} (u^r)^2 = 0, \\ \frac{d(u^r)^2}{dr} = 0. \end{array}\right\} \tag{25}$$

Using the condition (25), the equations (2), (23) and (24) together give the energy and angular momentum as

$$E^2 = \frac{\{16M^3r(3q^2 + 4Mr) - (q^2 + 4Mr)^3\}\{(q^2 + 4Mr)^2 - 32M^3r\}}{\{16M^3r(q^2 + 12Mr) - (q^2 + 4Mr)^3\}(q^2 + 4Mr)^2}, \tag{26}$$

and

$$L^2 = \frac{32M^3r^3(q^2 - 4Mr)}{16M^3r(q^2 + 12Mr) - (q^2 + 4Mr)^3}. \tag{27}$$

The circular geodesic exists when both energy and angular momentum are finite and real. For this, the denominators of equations (26) and (27) would be greater or equal to zero, i.e.,
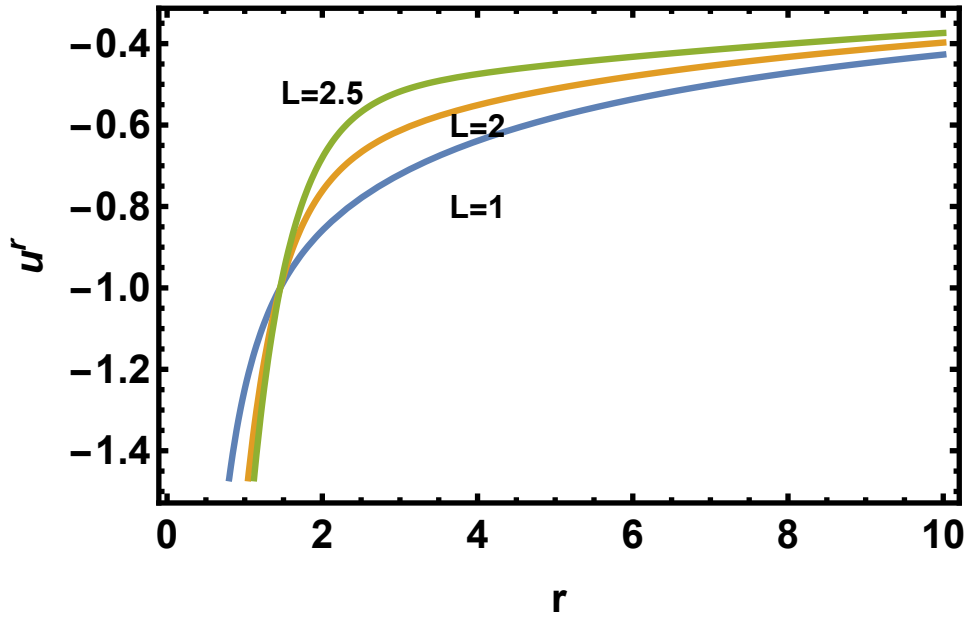
Figure 3: Plots of the radial component u^r for time-like geodesics w.r. to r for different values of L and q. (For interpretation of the references to color in this figure legend, the reader is referred to the web version of this article.)
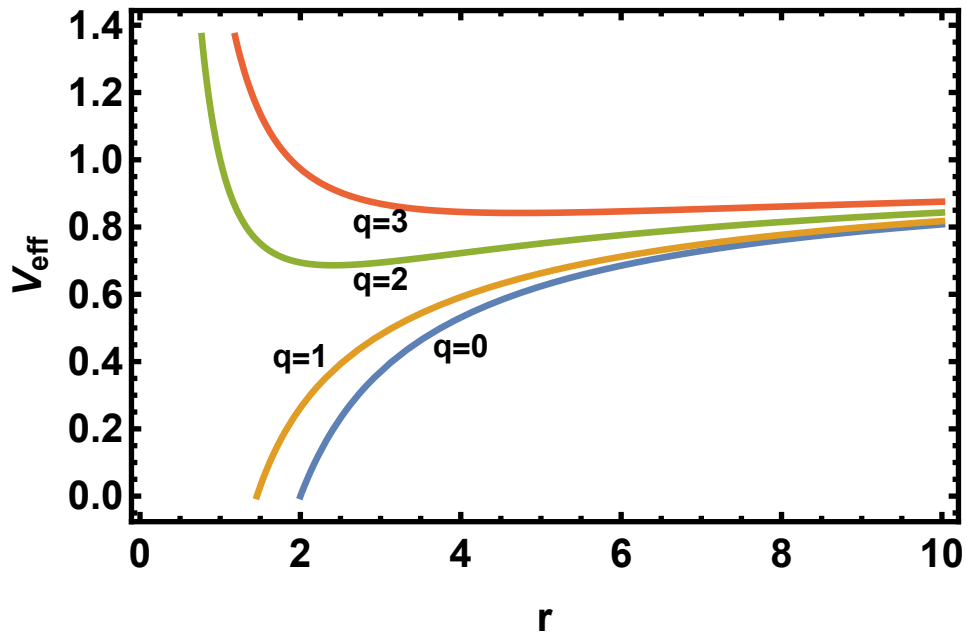
Figure 4: Plots of the effective potential V_{eff} for time-like geodesics w.r. to r for different values of L and q. (For interpretation of the references to color in this figure legend, the reader is referred to the web version of this article.)

$$16M^3r(q^2 + 12Mr) - (q^2 + 4Mr)^3 \geq 0,$$

or,

$$64M^3r^3 + 48M^2r^2(q^2 - 4M^2) + 4Mq^2r(3q^2 - 4M^2) + q^6 \geq 0.$$

and

$$q^2 + 4Mr \neq 0.$$

The minimum radius of time-like circular geodesics will be the radius of an unstable circular photon orbit.

One can obtain ISCO of this regular black hole using the condition (25) with an additional condition [39, 40, 41, 42, 43, 44, 45],

$$\frac{d^2(u^r)^2}{dr^2} = 0, \tag{28}$$

which is given by ISCO equation as

$$1024M^5r^5 + 256M^4r^4(7q^2 - 24M^2) + 768q^2M^3r^3(q^2 - 2M^2) + 64q^4M^2r^2(q^2 + 2M^2)$$
$$-4q^6Mr(5q^2 - 8M^2) - 3q^{10} = 0, \tag{29}$$

and MBCO equation as

$$16M^5r^2 + 16M^4r(q^2 - 4M^2) + 3q^4M^3 = 0. \tag{30}$$

Solving equations (29) and (30) we get ISCO radius $r = r_{ISCO}$ and MBCO radius $r = r_{MBCO}$ of this regular black hole. If $r > r_{ISCO}$, then we have stable circular orbits, and as well as if $r > r_{MBCO}$ then bounded spherical orbits are present for our charged regular black hole. When $q \to 0$ then from equations (29) and (30), we have $r_{ISCO} = 6M$ and $r_{MBCO} = 4M$, corresponding to Schwarzschild black hole.

4 Center-of-mass energy (CME) for particles collision

We classify this section into two parts depending on different types of particle collision near the horizon of this regular black hole. Here we take the equatorial plane throughout the geodesics motion for the particle collision. The four-velocity components for time-like geodesics are [38]

$$\left.\begin{array}{l} u^t = \dot{t} = \frac{E}{\mathrm{F}(r)}, \\ u^r = \dot{r} = \pm\sqrt{E^2 - \mathrm{F}(r)(1 + \frac{L^2}{r^2})}, \\ u^\theta = \dot{\theta} = 0, \\ u^\phi = \dot{\phi} = \frac{L}{r^2}. \end{array}\right\} \tag{31}$$

There should be $E^2 > \mathrm{F}(r)(1 + \frac{L^2}{r^2})$ for infall/escape of the particles. $u_r > 0$ describes outgoing geodesics, whereas $u_r < 0$ indicates incoming geodesics for the particles. To maintain this condition, we take a negative sign of u_r for the particles falling into our charged regular black hole. So, the corresponding three-velocity components (31) reduce to the form:

$$u_i^a = \left(\frac{E_i}{\mathrm{F}(r)}, -Z_i, 0, \frac{L_i}{r^2} \right), \tag{32}$$

where

$$Z_i = \sqrt{E_i^2 - \mathrm{F}(r)(1 + \frac{L_i^2}{r^2})}. \tag{33}$$

4.1   Two neutral particles with different masses

We calculate center-of-mass energy for two colliding particles whose rest masses are M_1 and M_2 respectively. We define CM energy formula as [38]

$$E_{CM}^2 = 2M_1 M_2 \left[\frac{(M_1 - M_2)^2}{2M_1 M_2} + (1 - g_{ab} u_1^a u_2^b) \right]. \tag{34}$$

Substituting equations (31), (32), (33) in equation (34) we get the CM energy as

$$E_{CM}^2 = 2M_1 M_2 \left[\frac{(M_1 - M_2)^2}{2M_1 M_2} + \left(1 + \frac{E_1 E_2}{\mathrm{F}(r)} - \frac{Z_1 Z_2}{\mathrm{F}(r)} - \frac{L_1 L_2}{r^2} \right) \right]. \tag{35}$$

We have drawn the plots of E_{CM} w.r.t. r for different values of L_1, L_2, M_1, M_2, q for different masses in Figs. 5 and 6. We see that E_{CM} decreases as r increases.
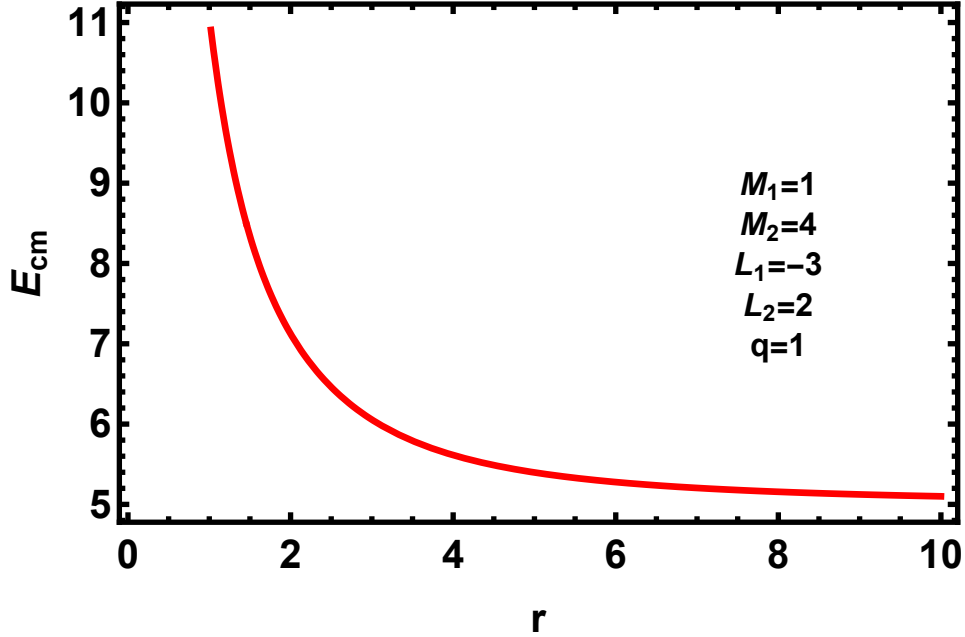
Figure 5: Plot of E_{CM} w.r.t. r.
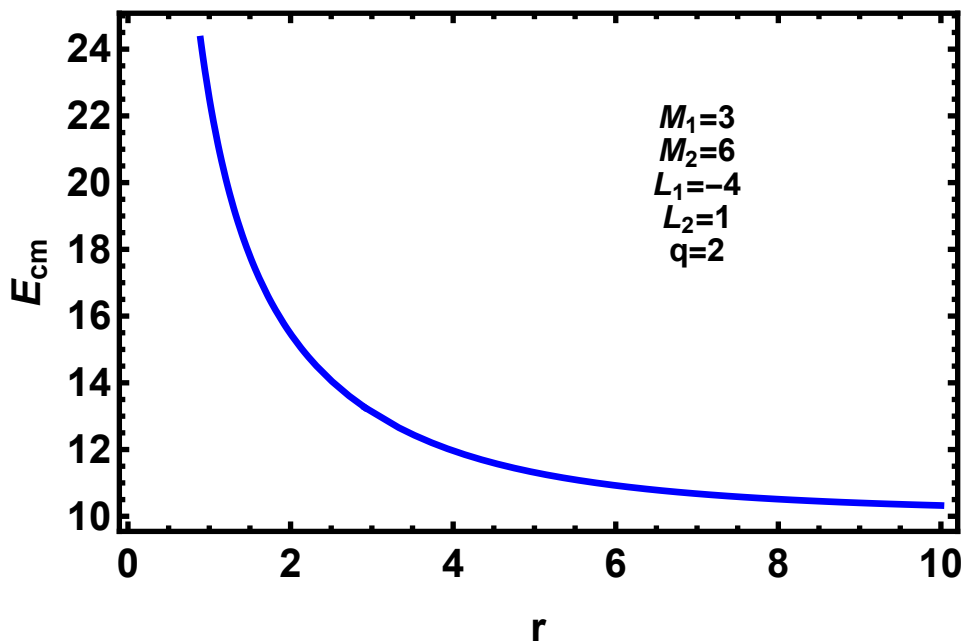
Figure 6: Plot of E_{CM} w.r.t. r.

4.2 Two neutral particles of same mass

We can follow the previous section for colliding particles whose rest masses are same as M. We define CM energy formula as [38]

$$\left(\frac{E_{CM}}{\sqrt{2}M}\right)^2 = 1 + \frac{E_1 E_2}{\mathrm{F}(r)} - \frac{Z_1 Z_2}{\mathrm{F}(r)} - \frac{L_1 L_2}{r^2}. \tag{36}$$

For non-extremal black hole (i.e., $r_+ \neq r_-$), then CM energy (36) near the event horizon reduces to the following form

$$E_{CM}|_{r=r_+} = \sqrt{2}M\sqrt{1 - \frac{L_1 L_2}{r_+^2}}. \tag{37}$$

The angular velocity of this regular black hole at $r = r_+$ is given as

$$\Omega_H = \frac{\dot{\phi}}{\dot{t}} = \frac{\sqrt{(q^2 + 4Mr)^2 - 32M^3 r}}{r(q^2 + 4Mr)}. \tag{38}$$

Then the critical angular momenta is written as

$$L_i = \frac{E_i}{\Omega_H}. \tag{39}$$

For extremal case, when $q^2 = 2M$ then the horizon is at $r = 0.5M$ and if one of particles has divergent angular momentum at the horizon i.e., $L_1 \to \infty$ as $r \to 0.5M$, then we get infinite CM energy ($E_{CM} \to \infty$). At the center of this black hole ($r = 0$), the center-of-mass also diverges. Again $E_{CM} \to 2M^2$ as $r \to \infty$. We have drawn the plots of E_{CM} w.r.t. r for different values of L_1, L_2, M, q for same mass in Figs. 7 and 8. We see that E_{CM} decreases as r increases.
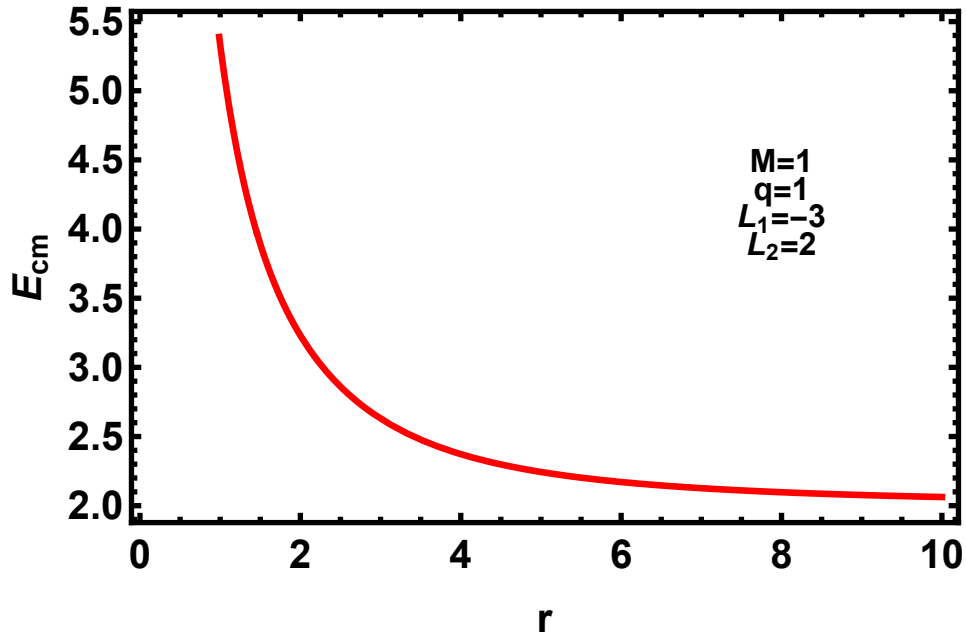
Figure 7: Plot of E_{CM} w.r.t. r.
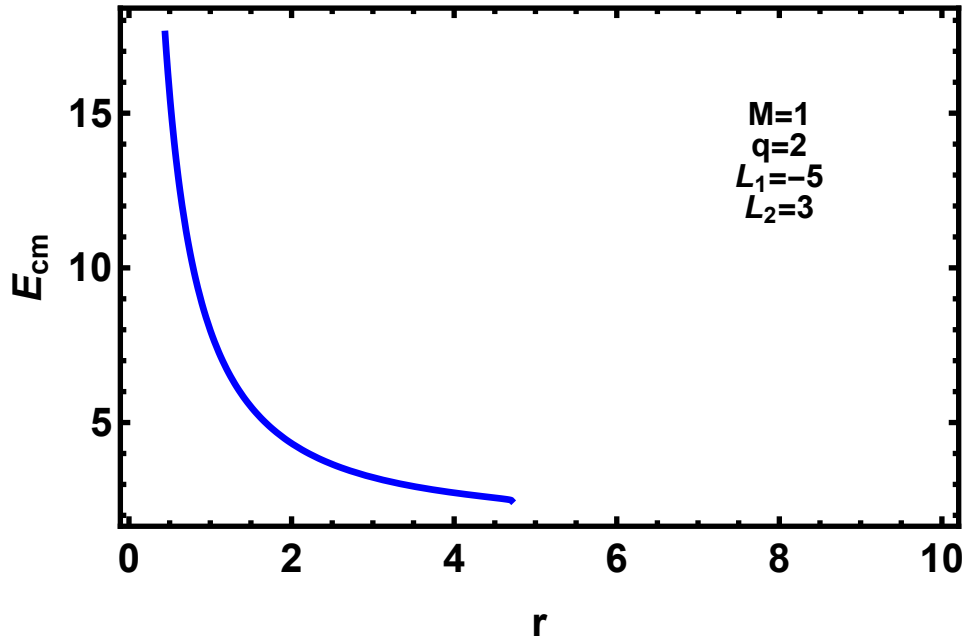
Figure 8: Plot of E_{CM} w.r.t. r.

5   Particle collisions with photon

Due to Hawking radiation, we follow the Compton scattering process. Here we consider an infalling particle collision with a demonstrative massless photon near the horizon in the

equatorial plane ($\theta = \frac{\pi}{2}$) of this regular black hole [46]. Let us assume four velocities of particle and photon are $(U^t, U^r, U^\theta, U^\phi)$ and $(K^t, K^r, K^\theta, K^\phi)$ respectively where $U^\theta = K^\theta = 0$ for equatorial plane. The time-like geodesic of a particle and the null geodesic of a photon satisfy [46]

$$g_{\mu\nu}U^\mu U^\nu = -1,$$

and

$$g_{\mu\nu}K^\mu K^\nu = 0,$$

respectively. The particle velocity components are same as equation (31) and the photon velocity components (with $\sigma = 0$) are given as

$$K^t = \frac{E_\gamma}{\mathrm{F}(r)}, \tag{40}$$

$$K^\phi = \frac{L_\gamma}{r^2}, \tag{41}$$

$$(K^r)^2 = E_\gamma^2 - \frac{L_\gamma^2}{r^2}\mathrm{F}(r), \tag{42}$$

where $\mathrm{F}(r)$ is given by equation (2) and E_γ, L_γ are respectively the energy and angular momentum of the photon. Now the center-of-mass for the collision of a particle of rest mass m with a massless photon in the equatorial plane can be calculated as [46]

$$E_{cm}^2 = m^2 - 2mg_{\mu\nu}U^\mu K^\nu. \tag{43}$$

Using equations (31), (40), (41) and (42), the equation (43) can be reduced to

$$E_{cm}^2 = m^2 - 2m\left[-\frac{EE_\gamma}{\mathrm{F}(r)} + \frac{\sqrt{E^2 - \mathrm{F}(r)\left(1 + \frac{L^2}{r^2}\right)}\sqrt{E_\gamma^2 - \frac{L_\gamma^2}{r^2}\mathrm{F}(r)}}{\mathrm{F}(r)} + \frac{LL_\gamma}{r^2} \right]. \tag{44}$$

We draw the plots of E_{CM} w.r.t. r for different values of M, L, L_γ, q for particle-photon collision in Figs. 9 and 10. We see that E_{CM} decreases as r increases.

6   Collision between two photons

Motivated by Halilsoy and Ovgun [46] we are interested in considering the collision of two massless photons near the horizon in the equatorial plane ($\theta = \frac{\pi}{2}$) of this regular black hole. The null geodesic of two photons satisfy

$$g_{\mu\nu}K^\mu K^\nu = 0.$$

The photon velocity components (with $\sigma = 0$) are given as

$$K_i^t = \frac{E_{\gamma_i}}{\mathrm{F}(r)}. \tag{45}$$

$$K_i^\phi = \frac{L_{\gamma_i}}{r^2}. \tag{46}$$
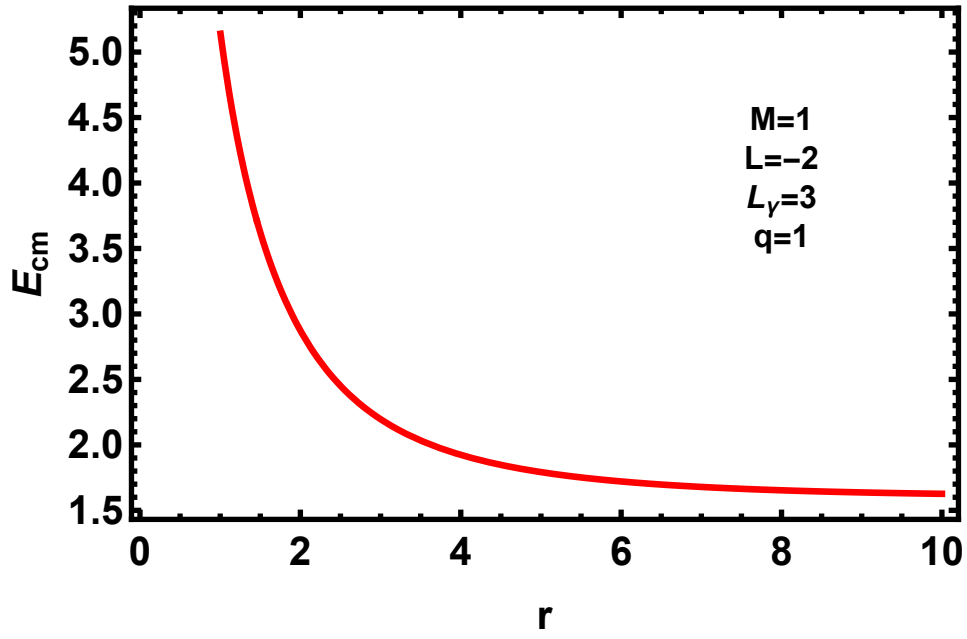
Figure 9: Plot of E_{CM} w.r.t. r for particle-photon collision.
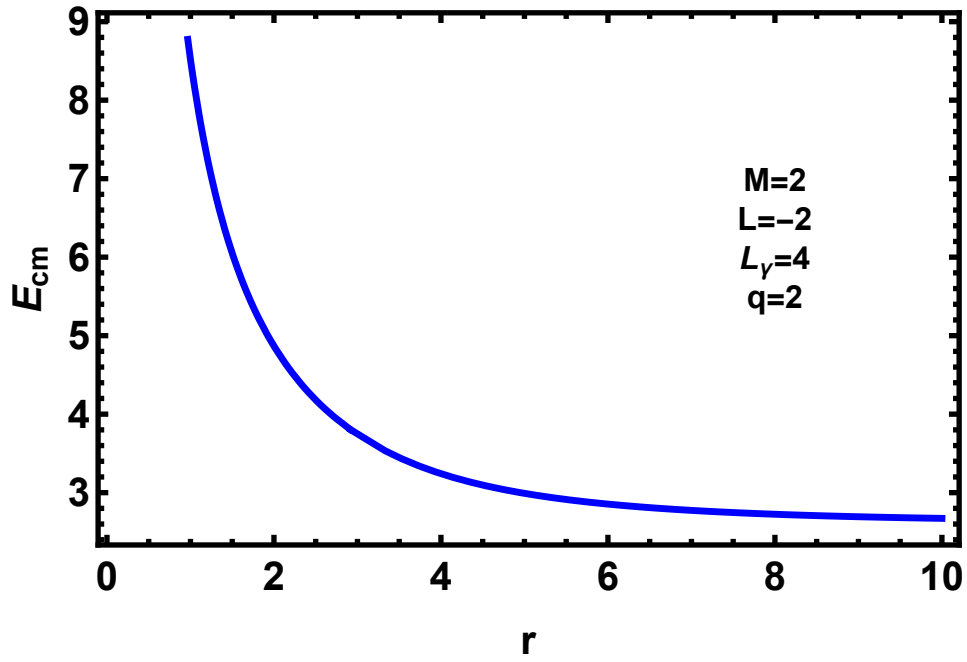
Figure 10: Plot of E_{CM} w.r.t. r for particle-photon collision.

$$(K_i^r)^2 = E_{\gamma_i}^2 - \frac{L_{\gamma_i}^2}{r^2}\mathrm{F}(r). \tag{47}$$

$$K_i^\theta = 0, \tag{48}$$

where F(r) is given by equation (2) and E_{γ_i}, L_{γ_i} are energy and angular momentum of the ith photon respectively where $i = 1, 2$. Now the center of mass for collision of two mass free photons in equatorial plane can be calculated as [46]

$$E_{cm}^2 = -2g_{\mu\nu}K_1^\mu K_2^\nu. \tag{49}$$

Using equations (45), (46) and (47), the equation (49) can be reduced to

$$E_{cm}^2 = -2\left[-\frac{E_{\gamma_1}E_{\gamma_2}}{F(r)} + \frac{\sqrt{E_{\gamma_1}^2 - \frac{L_{\gamma_1}^2}{r^2}F(r)}\sqrt{E_{\gamma_2}^2 - \frac{L_{\gamma_2}^2}{r^2}F(r)}}{F(r)} + \frac{L_{\gamma_1}L_{\gamma_2}}{r^2} \right]. \tag{50}$$

We draw the plots of E_{CM} w.r.t. r for different values of $M, L_{\gamma_1}, L_{\gamma_2}, q$ for photon-photon collision in Figs. 11 and 12. We see that E_{CM} decreases as r increases.
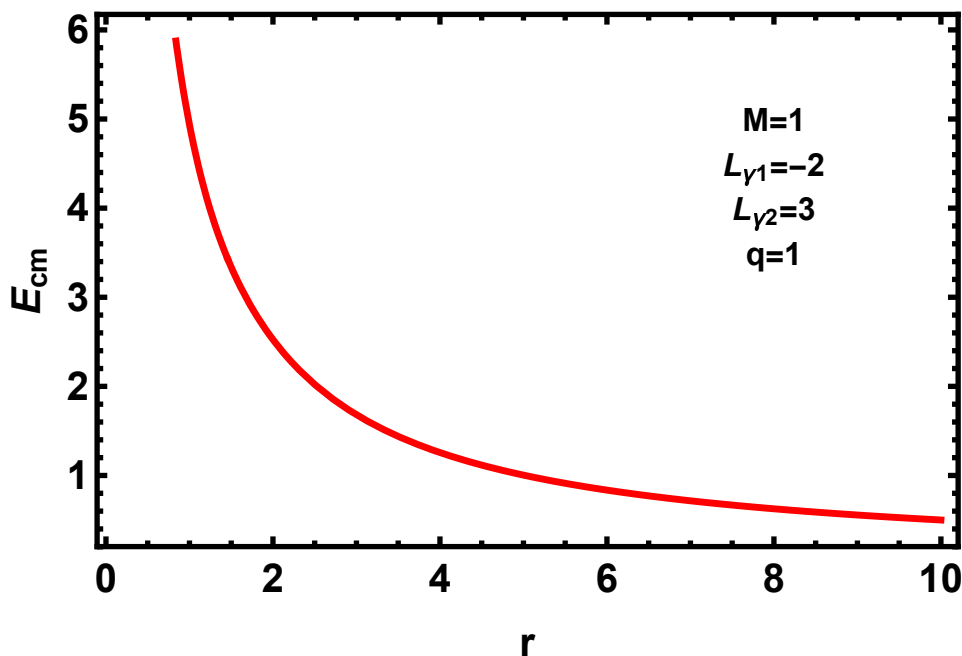
Figure 11: Plots of E_{CM} w.r.t. r for photon-photon collision.

7   Discussions

In this work, we have considered a static spherically symmetric charged non-singular (regular) black hole. Then we have found the radii of the Cauchy horizon and event horizon. After that, we have studied the geodesics of circular orbits, i.e., ISCO and MBCO of this regular black hole. We have found the effective potential and energy for null and time-like geodesics. For null geodesic, we have obtained the impact parameter ($D = E/L$). Next, we have investigated center-of-mass energy (CME) near the horizons of the regular black hole with particle collision, and we noticed that the CME is infinite for the extremal case
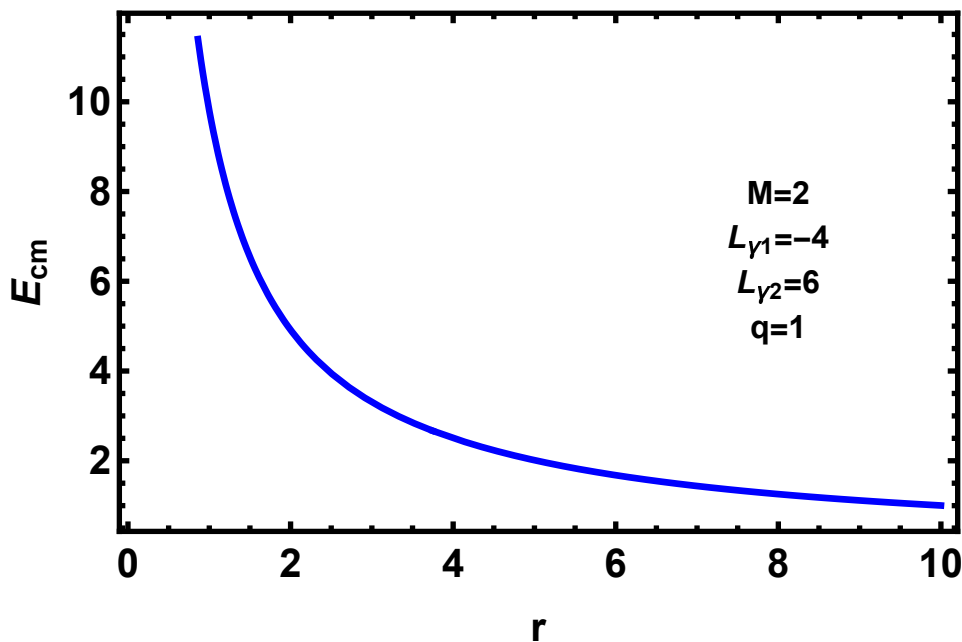
Figure 12: Plots of E_{CM} w.r.t. r for photon-photon collision.

and finite for the non-extremal case with the same mass particle collision. The center-of-mass energy is divergent near the center of the black hole and $E_{CM} \to 2M^2$ when $r \to \infty$. From the Compton process, we carried out research on finding the CME for particle-photon collision and photon-photon collision in the background of this regular black hole. In all collisions, we have observed that CME decreases as r increases from the black hole.

References

[1] M. Banados, J. Silk and S. M. West, "Kerr Black Holes as Particle Accelerators to Arbitrarily High Energy", Phys. Rev. Lett. **103**, 111102 (2009).

[2] T. Jacobson and T. P. Sotiriou, "Spinning Black Holes as Particle Accelerators", Phys. Rev. Lett. **104**, 021101 (2010).

[3] K. Lake, "Particle Accelerators inside Spinning Black Holes", Phys. Rev. Lett. **104**, 211102 (2010).

[4] Oleg B. Zaslavskii, "Acceleration of particles by nonrotating charged black holes", JETP Lett. **92**, 571-574 (2010).

[5] S. W. Wei, Y. X. Liu, H. Guo and C. E. Fu, "Charged spinning black holes as particle accelerators", Phys. Rev. D **82**, 103005 (2010).

[6] Yang Li, Jie Yang, Yun-Liang Li, Shao-Wen Wei, Yu-Xiao Liu, "Particle Acceleration in Kerr (anti-) de Sitter Black Hole Backgrounds", Class. Quant. Grav. **28**, 225006 (2011).

[7] C. Liu, S. Chen, C. Ding and J. Jing, "Particle acceleration on the background of the Kerr-Taub-NUT spacetime", Phys. Lett. B **701**, 285 (2011).

[8] Yi Zhu, Shao-Feng Wu, Yu-Xiao Liu, Ying Jiang, "General stationary charged black holes as charged particle accelerators",Phys. Rev. D **84**, 043006 (2011).

[9] J. L. Said and K. Z. Adami,"Large-scale structure in f(T) gravity", Phys. Rev. D **83**, 104047 (2011).

[10] A. Abdujabbarow, B. Ahmedov, B. Ahmedov,"Energy extraction and particle acceleration around a rotating black hole in Hoava-Lifshitz gravity", Phys. Rev. D **84**, 044044 (2011).

[11] J. Sadeghi, B. Pourhassan, "Particle acceleration in Horava-Lifshitz black holes", Eur. Phys. J. C **72**, 1984 (2012).

[12] J. Sadeghi, B. Pourhassan, H. Farahani,"Rotating Charged Hairy Black Hole in (2+1) Dimensions and Particle Acceleration", Commun. Theor. Phys. **62**, no. 3, 358-362 (2014).

[13] M. Patil, P. S. Joshi,"Particle acceleration by Majumdar-Papapetrou di-hole", Gen. Rel. Grav. **46**, no. 10, 1801 (2014).

[14] P. Pradhan,"String black holes as particle accelerators to arbitrarily high energy", Astrophys. Space Sci. 352, 129-134 (2014).

[15] P. Pradhan,"Charged dilation black holes as particle accelerators", Astropart. Phys. **62**, 217-229 (2015).

[16] T. Harada, M. Kimura,"Black holes as particle accelerators: a brief review", Class. Quant. Grav. **31**, 243001 (2014).

[17] P. Pradhan, "Regular Black Holes as Particle Accelerators", arXiv:1402.2748 [gr-qc].

[18] G. Abbas, U. Sabiullah,"Geodesic study of regular Hayward black hole", Astrophys. Space Sci. **352**, 769 (2014).

[19] C. Bambi and L. Modesto,"Rotating regular black holes", Phys. Lett. B **721**, 329 (2013).

[20] R. M. Wald, "Gravitational Collapse and Cosmic Censorship", gr-qc/9710068.

[21] J. Jhingan, G. Magli, "Gravitational collapse of fluid bodies and cosmic censorship: analytic insights", gr-qc/9903103.

[22] J. Bardeen, "Non-singular general-relativistic gravitational collapse", Proceedings of International Conference GR5, Tbilisi, USSR (1968), p. 174.

[23] Ayon-Beato, A. Garcia, "Regular Black Hole in General Relativity Coupled to Nonlinear Electrodynamics", Phys. Rev. Lett. **80**, 5056 (1998).

[24] S. A. Hayward, "Formation and Evaporation of Nonsingular Black Holes", Phys. Rev. Lett. **96**, 031103 (2006).

[25] M. Amir and S. G. Ghosh, "Rotating Hayward's regular black hole as particle accelerator", JHEP **2015**, 015 (2015).

[26] P. Saha and U. Debnath, "Collision of particles near charged MSW black hole in 2 + 1 dimensions", Mod. Phy. Lett. A **34**, 1950127 (2019).

[27] P. Pradhan, "Charged dilaton black holes as particle accelerators", Astropart. Phys. **62**, 217 (2015).

[28] I. Dymnikova, "Cosmological term as a source of mass", Class. Quant. Grav. **19**, 725 (2002).

[29] L. Balart and E. C. Vagenas, "Regular black holes with a nonlinear electrodynamics source", Phys. Rev. D **90**, 124045 (2014).

[30] L. Balart and E. C. Vagenas, "Regular black hole metrics and the weak energy condition", Phys. Lett. B **730**, 14 (2014).

[31] P. Nicolini, A. Smailagic and E. Spallucci, "Noncommutative geometry inspired Schwarzschild black hole", Phys. Lett. B **632**, 547 (2006).

[32] S. Ansoldi, P. Nicolini, A. Smailagic and E. Spallucci, "Noncommutative geometry inspired charged black holes", Phys. Lett. B **645**, 261 (2007).

[33] E. Elizalde and S. R. Hildebrandt, "Family of regular interiors for nonrotating black holes with $T_0^0 = T_1^1$", Phys. Rev. D **65**, 124024 (2002).

[34] O. B. Zaslavskii, "Regular black holes and energy conditions", Phys. Lett. B **688**, 278 (2010).

[35] S. Chandrasekhar, "The Mathematical Theory of Black Holes", Clarendon Press, Oxford (1983).

[36] J. B. Hartle , "Gravity-An Introduction To Einstein's General Relativity", Benjamin Cummings (2003).

[37] M. Sharif and N. Haider, "Center-of-mass energy for the Plebanski-Demianski black hole", J. Theor. Exp. Phys. **117**, 78 (2013).

[38] A. Zakria and M. Jamil, "Center of Mass Energy of the Collision for Two General Geodesic Particles Around a Kerr-Newman-Taub-NUT Black Hole", JHEP **05**, 147 (2015).

[39] S. A. Kaplan, "On Circular orbits in Einsteinian Gravitation theory", J. Exp. Theor. Phys. **19**, 951 (1949).

[40] P. I. Jefremov, O. Y. Tsupko and G. S. B. Kogan, "Innermost stable circular orbits of spnning test particles in Schwarzschild and Kerr space-times", Phys. Rev. D **91**, 124030 (2015).

[41] Y. P. Zhang, S. W. Wei, W. D. Guo, T. T. Sui and Y. X. Liu, "Innermost stable circular orbit of spinning particle in charged spinning black hole background", Phys. Rev. D **97**, 084056 (2018).

[42] C. Chakraborty, "Inner-most stable circular orbits in extremal and non-extremal Kerr-Taub-NUT spacetimes", Eur. Phys. J. C **74**, 2759 (2014).

[43] S. Hod, "Self-gravitating ring of matter in orbit around a black hole: the innermost stable circular orbit", Eur. Phys. J. C **74**, 2840 (2014).

[44] J. M. Bardeen, W. H. Press and S. A. Teukolsky, "Rotating Black Holes: Locally Non-rotating Frames, Energy Extraction, and Scalar Synchrotron Radiation", Astrophys. J. **178**, 347 (1972).

[45] S. Hod, "Marginally bound (critical) geodesics of rapidly rotating black holes", Phys. Rev. D **88**, 087502 (2013).

[46] M. Halilsoy and A. Ovgun, "Particle acceleration by static black holes in a model of $f(R)$ gravity", Canadian Journal of Physics **95**, 1037 (2017).